

Layered Calcium Structures of *p*-Phosphonic Acid *O*-Methyl-Calix[6]areneThomas E. Clark,[†] Adam Martin,[†] Mohamed Makha,[†] Alexandre N. Sobolev,[†] Dian Su,[‡] Henry W. Rohrs,[‡] Michael L. Gross,[‡] and Colin L. Raston*[†][†]Centre for Strategic Nano-Fabrication, School of Biomedical, Biomolecular and Chemical Sciences, University of Western Australia, 35 Stirling Highway, Crawley, Western Australia 6009, Australia, and [‡]Department of Chemistry, Washington University, St. Louis, Missouri 63130

Received March 17, 2010; Revised Manuscript Received May 6, 2010

ABSTRACT: Hexamethoxy-calix[6]arene has been fully functionalized with *p*-phosphonic acid groups on the upper rim in 57% yield over three steps and has been authenticated in the solid state by X-ray diffraction as either a nitrate salt or one of two calcium complexes. The latter differ by the ratio of calcium ions per calixarene, either 3:1 or 4:1. In both structures, the coordination sphere of the calcium ions is made up of oxygen atoms from the phosphonic acid groups and from water of crystallization, as part of extended polymeric layers in the extended three-dimensional packing. Hirshfeld surface analysis shows extensive O···H and O···Ca interactions for the phosphonic acid moieties in both calcium structures. Matrix assisted laser desorption ionization time-of-flight mass spectrometry (MALDI-TOF-MS) of the hexaphosphonic acid shows nanoarrays consisting of up to a maximum of 28 calixarene units.

Introduction

Calixarenes are a class of macrocyclic compounds that have been utilized in a wide variety of roles, including sensors,¹ gas absorption,² and the encapsulation of guest molecules, be it organic molecules such as fullerenes³ or ions such as the lanthanides.⁴ The main reason for the wide variety of uses for calixarenes is due in part to their ease of functionalization, and the attachment of acidic groups at the upper rim is an important strategy in self-assembly studies, for example, using sulfonic acid/sulfonate groups which affords a remarkable diverse range of structures.⁵ Attachment of alkyl chains to the lower rim of calixarenes allows the formation of bilayers of differing thicknesses,⁶ which in combination with polar head groups imparts lipophilic character onto the calixarenes. Another reason for the wide use of calixarenes is their relative ease of preparation, with calix[4, 6, and 8]arene accessible in large quantities in high yields.⁷

Calixarenes bearing phosphonic acid/phosphonate groups in the *para*-position at the upper rim are relatively new, further highlighting the diversity of calixarenes in general and are available in good yield, 62–68% overall for calix[4, 5, 6, and 8]arene involving robust five-step procedures.⁸ These calixarenes are water-soluble and form bilayers in the solid state, held together by strong hydrogen bonding between the diprotic phosphonic acid groups, and in solution and the gas phase they can form nanorafts.⁸ *O*-Alkylation at the lower rim while maintaining the integrity of the phosphonic acid/phosphate groups has also been reported, for methyl, *n*-butyl, and *n*-octadecyl chains.⁹ The methyl-substituted phosphonic acid calix[4]arene binds Cs⁺ ions in a 1,3-alternate conformation, through Cs···O and Cs··· π interactions.

Calcium(II) ions play an important role in biological functions, with calcium channels thought to be involved in Alzheimer's disease¹⁰ and certain cancers that increase the amount of calcium in the body through hypercalcemia.¹¹ *p*-Phosphonic acid calix[4]arene, devoid of *O*-alkyl groups, has been shown to

bind Ca²⁺ ions in the solid state,¹² and herein we show that phosphonic acid calix[6]arene bearing *O*-methyl groups at the lower rim binds Ca²⁺ ions, crystallizing in the classical “double partial cone” conformation for calix[6]arenes in general.

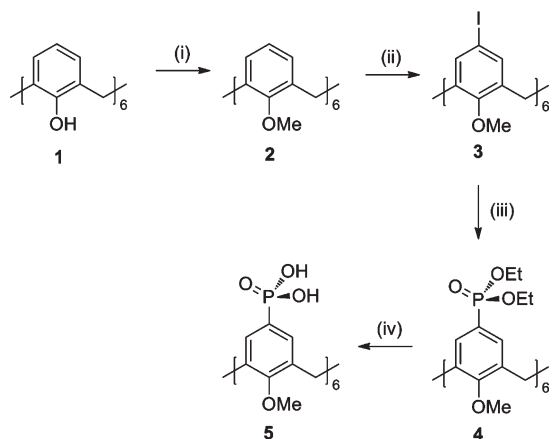
Hirshfeld surface analysis is a technique that is finding a plethora of uses in analyzing intermolecular contacts and interactions of larger molecules,¹³ including for example, both alkyl esters of phosphonated calixarenes,^{6a} and phosphonic acid analogues.¹² The parameter d_{norm} is of particular interest in undertaking Hirshfeld surface analyses, as it can be easily discerned, using a red-white-blue color scheme, which contacts are shorter or longer than the sum of the van der Waals radii of the atoms, and thus identify close contacts in the structure.¹⁴ The fingerprint plots are also very useful, as they can be used to identify specific contacts, such as CH··· π contacts, which have characteristic shapes and positions on the plots.¹⁴

Results and Discussion

The synthesis of *p*-phosphonic acid hexamethoxy-calix[6]arene, **5**, was accomplished in four steps starting from calix[6]arene **1**, Scheme 1. Alkylation of **1** using MeI and NaH in dimethylformamide gave methoxycalix[6]arene, **2**, which was subsequently iodinated using CF₃CO₂Ag and I₂ in chloroform affording **3** in 66% yield. The iodinated precursor, **3**, was phosphorylated using P(OEt)₃ and NiCl₂ in benzonitrile to give the phosphonate ester **4** in 92% yield. De-esterification of **4** using Me₃SiBr in acetonitrile gave the target phosphonic acid **5** in 95% yield.

Single crystal X-ray diffraction was used to authenticate calixarenes **4** and **5** as complexes **4a** and **5a–c**, respectively. The crystalline complex **4a** was prepared by slow evaporation of a saturated solution of **4** in toluene over 5 days to yield complex **4a** as **4**·H₂O. Complex **5a** was prepared by slow evaporation of a saturated solution of **5** in MeOH/6 M HNO₃/CsNO₃ over 7 days to yield complex **5a** as **5**·4HNO₃·6H₂O. Slow evaporation of a solution of **5** with three or four equivalents of calcium acetate affords complex **5b** as **5**⁶⁻·3Ca²⁺·28H₂O and complex **5c** as **5**⁸⁻·4Ca²⁺·261/2H₂O,

*To whom correspondence should be addressed. E-mail: colin.raston@uwa.edu.au.

Scheme 1. Synthetic Procedure for *p*-Phosphonic Acid Hexamethoxy-calix[6]arene^a


^a (i) MeI/NaH/DMF, (ii) CF₃CO₂Ag/I₂/CHCl₃, (iii) P(OEt)₃/NiCl₂/PhCN, (iv) BTMS/MeCNMe = methyl, Et = ethyl, Ph = phenyl, BTMS = bromotrimethylsilane, DMF = dimethylformamide.

respectively. Only complexes **5b** and **5c** will be described in detail herein.

Complex **5b** crystallizes in the space group $P\bar{1}$ ($Z=2$) with the asymmetric unit comprising two separate halves of two calixarene molecules located at two different inversion centers (0, 0, 1/2 and 1/2, 1/2, 0), 3 calcium atoms, and 28 crystalline water molecules, Figure 1. According to our conventional atomic numbering scheme the aromatic rings 1–3 belong to calixarene A, and aromatic rings 4–6 belong to calixarene B. The coordination sphere of two of the calcium atoms (Ca1 and Ca3) consist of four crystalline water molecules and three (directly or symmetry connected) oxygen atoms from the *p*-phosphonic acid moieties of calixarene A, Ca–O distances 2.310(2)–2.534(2) Å, and calixarene B, Ca–O distances 2.258(2)–2.557(2) Å. The third calcium atom (Ca2) is seven-coordinated and involves two oxygen atoms from different calixarene molecules and five water molecules into its coordination sphere, Ca–O distances 2.326(2)–2.559(2) Å. This combination of interactions between calixarene molecules and calcium atoms forms a continuous polymeric monolayer along the [111] direction in the overall crystal packing, Figure 2.

All of the crystalline water molecules are involved in an H-bond network with O···O distances in the range of 2.522(3)–3.209 Å. The 3D packing of the molecules in the crystal has a sandwich structure with layers of the calixarene molecules alternated with layers of the Ca/water environment extended along the *a*-axis in crystal, Figure 2. The conformation of the calixarene molecules, A and B, are remarkably similar and can be described as a container macrocycle, Figure 3. For calixarene A, a side wall is formed by the parallel-oriented aromatic rings 1 and 2 in the form of parallelepiped and with ring 3 at the top and bottom of the container. The dihedral angles between the middle-cross plane (0) of calixarene A and the aromatic rings are 86.3(1) (planes 0-1), 87.6(1) (0-2), 28.2(1) (0-3), and 75.0(1)° (1-2). The corresponding values calculated for calixarene B are 87.3(1) (0-4), 88.8(1) (0-5), 28.7(1) (0-6), and 77.1(1)° (4-5). In addition to the H-bonds, there are no specific interactions between the calixarene molecules.

Complex **5c** crystallizes in the space group $P\bar{1}$ ($Z=1$) with the asymmetric unit comprising one calixarene molecule situated at an inversion center (1/2, 1/2, 1/2), two calcium atoms, 13 fully occupied water molecules, and one-half occupied

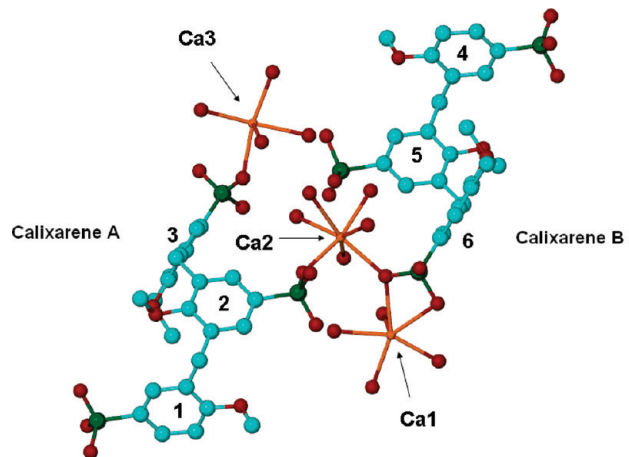


Figure 1. Ball and stick representation of the asymmetric unit for complex **5b** showing the coordination spheres of the calcium ions. Hydrogen atoms and non-calcium coordinated water molecules have been omitted for clarity. For all crystallographic figures, the following color scheme is used; blue for carbon atoms, green for phosphorus atoms, red for oxygen atoms, gold for calcium atoms, and silver for hydrogen atoms.

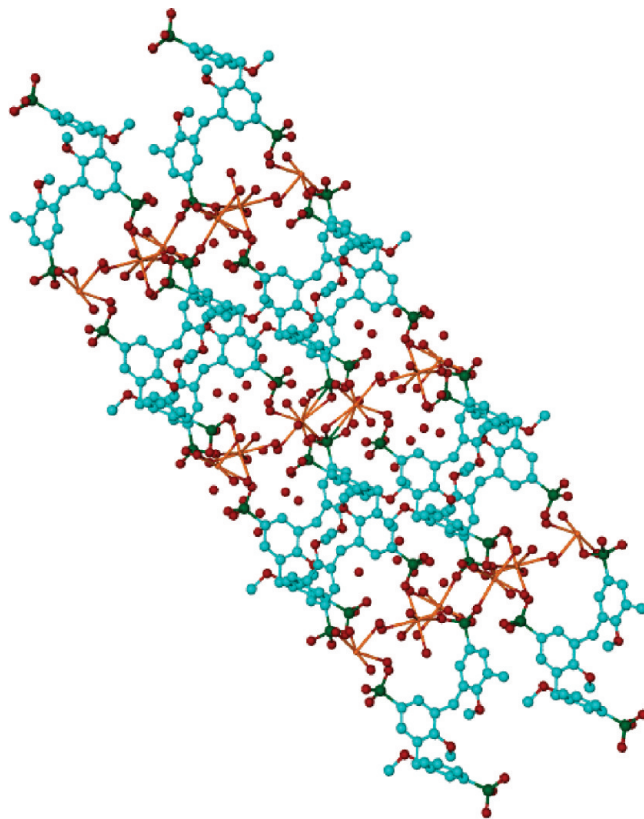


Figure 2. Projection of the overall packing for complex **5b** along the [111] direction showing the continuous polymeric monolayer. Hydrogen atoms have been omitted for clarity.

water molecule, Figure 4. The container conformation of the calixarene molecule is similar to that described above for the calixarene molecules in complex **5b**. The dihedral angles between middle-cross plane (0) of the calixarene and aromatic rings are 89.1(1) (planes 0-1), 86.9(1) (0-2), 20.4(2) (0-3), and 71.0(1)° (1-2). One of the *p*-phosphonic acid moieties and its symmetry equivalent are completely deprotonated, making the total charge of the calixarene equal to -8 .

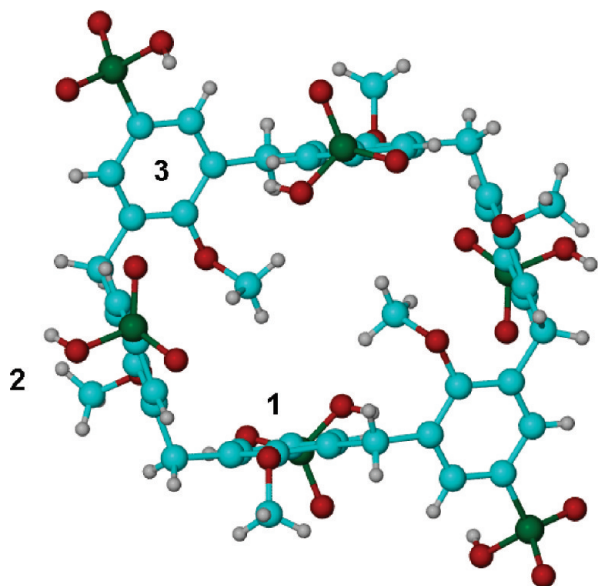


Figure 3. View of the container for calixarene A with aromatic rings 1–3 numbered.

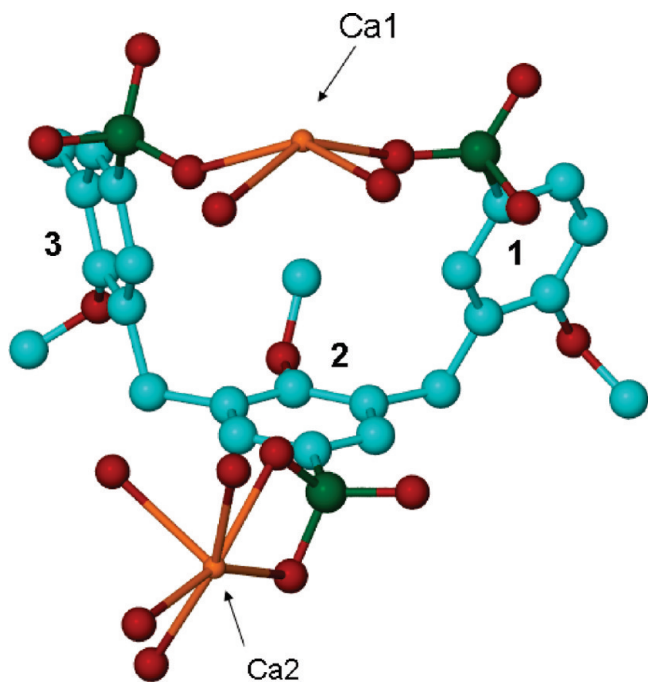


Figure 4. Ball and stick representation of the asymmetric unit for complex **5c**. Hydrogen atoms and noncalcium coordinated water molecules have been omitted for clarity.

The coordination spheres of the calcium are different, with Ca1 eight coordinate through five water molecules and three oxygen atoms from the *p*-phosphonic acid moieties of the calixarene, with two water molecules bridging Ca1–Ca1 atoms to form a polymeric chain. Ca2 is seven coordinate with four crystalline water molecules and three oxygen atoms belonging to *p*-phosphonic acid groups, with two water molecules bridging Ca2–Ca1 atoms to complete the polymeric chain. This is associated with the calixarene molecules being linked in an extended polymeric layer, parallel to the *c*-axis with Ca–O distances in the range of 2.293(3)–2.817(4) Å, Figure 5. The 3D-packing of the molecules is effectively a

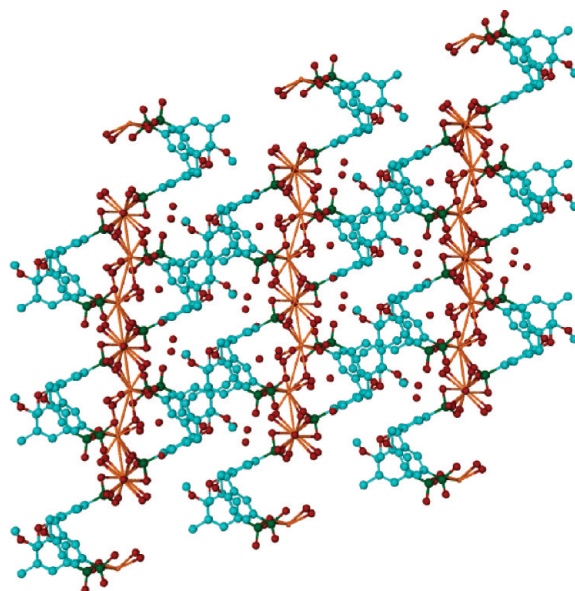


Figure 5. Projection of the overall packing for complex **5c** as viewed down the *b* axis showing the extended polymeric layer.

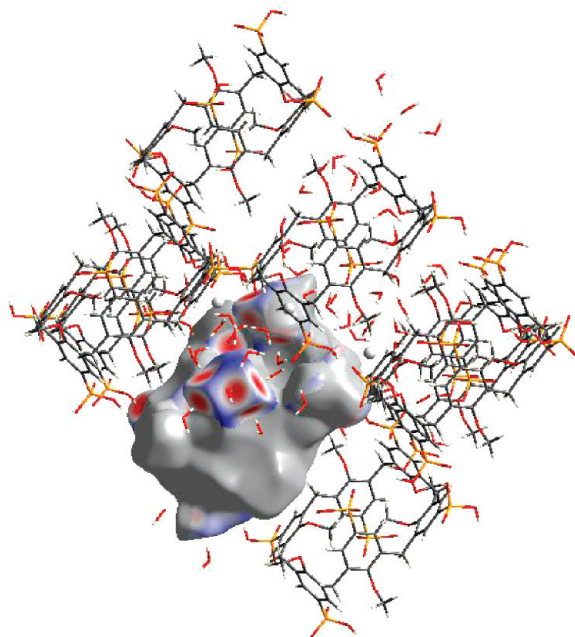


Figure 6. View of the O...H interactions for calixarene B in complex **5b**, with red areas highlighting short contacts.

sandwich structure with layers of the calixarene molecules alternating with layers of Ca/water moieties, extended parallel to the *a*–*b* plane. There are water molecules and hydroxyls of phosphonic groups involved in a H-bond network with O...O distances, 2.476(4)–3.271(5) Å.

Hirshfeld surface analysis was performed on complexes **5b** and **5c** in order to gain insight into the nature of the intermolecular interactions within the crystal structures. Both molecules of the phosphonated calix[6]arene in the asymmetric unit of **5b** show similar C...H contacts, which make up 7.3 and 7.2% of the Hirshfeld surface for calixarene A and calixarene B, respectively. These contacts represent CH... π acceptor contacts and are caused by the O-methyl group of a neighboring calixarene pointing toward a phenyl ring of calixarene A or B.

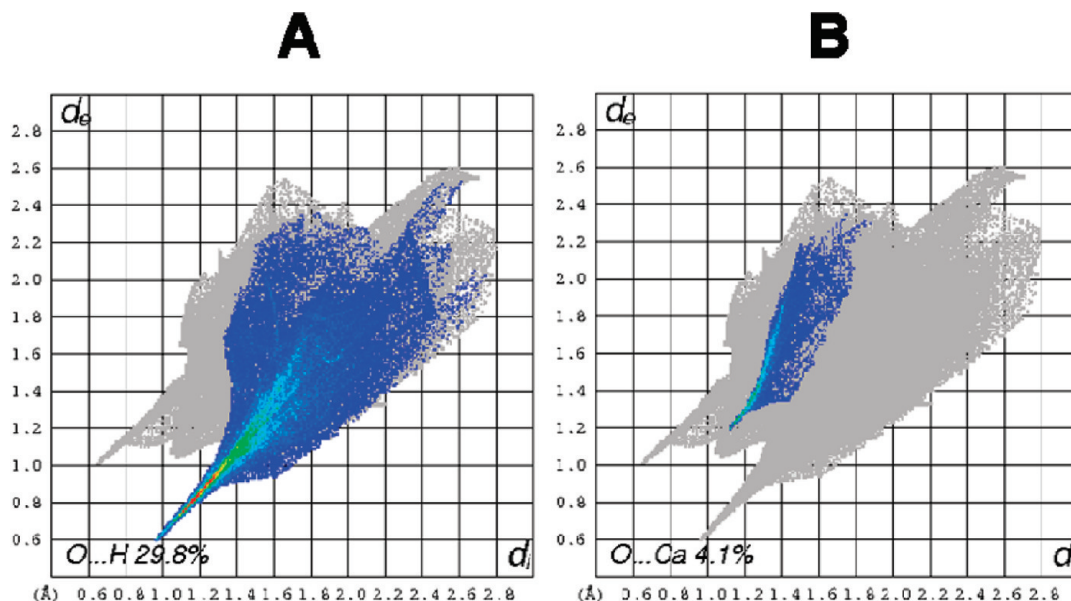


Figure 7. Fingerprint plots of calixarene B in complex **5b**: (A) O \cdots H interactions and (B) O \cdots Ca interactions.

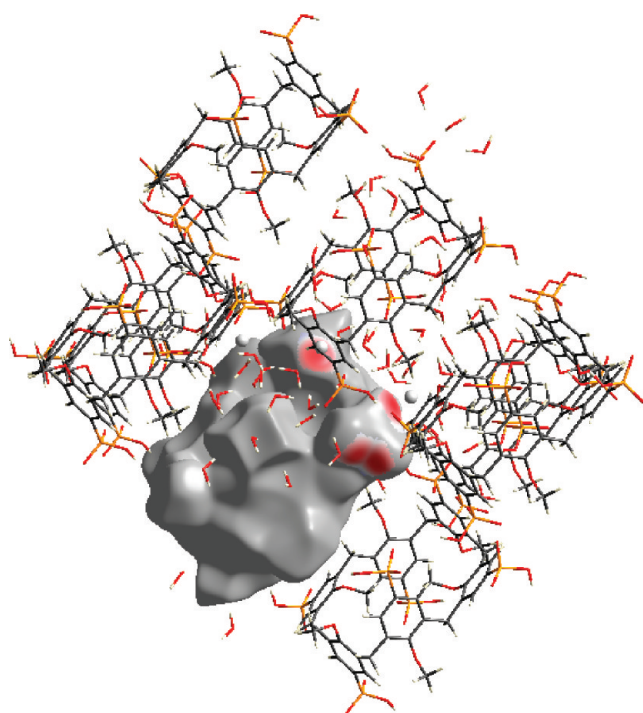


Figure 8. View of the O \cdots Ca interactions for calixarene B in complex **5b**, with red areas highlighting short contacts.

A large portion of the interactions that comprise the Hirshfeld surface of the calixarenes in **5b** are due to O \cdots H interactions which are quite similar for both molecules, Figure 6. Of the six phosphonate groups present at the upper rim of the calixarene, four are involved in O \cdots H interactions. Where there are deprotonated phosphonate ligands present in the structure, they interact solely with water molecules. There are points in the expanded structure where phosphonate groups are in close proximity to each other, in which case they are bridged by a water molecule. Other interactions also involve contacts between water molecules and the phenolic oxygen of the calix-[6]arenes, and O \cdots H interactions make up 29.5 and 29.8% of the surface for calixarene A and B, respectively, and can be

viewed as a spike in the bottom left-hand corner of the fingerprint plot, Figure 7A.

Interestingly, the two phosphonate groups that do not show strong O \cdots H interactions display strong O \cdots Ca interactions instead, Figure 8. These O \cdots Ca interactions appear on the fingerprint plot as a bright streak between the O \cdots H and H \cdots O spikes, and they make up 4.1 and 4.0% of the surface respectively for calixarenes 1 and 2, Figure 7B. Also for the phosphonic acid groups that have O \cdots Ca interactions, every oxygen atom in that group, be it from a formal P \cdots O double bond, protonated or deprotonated hydroxyl group, interacts with a unique calcium atom.

Of the four phosphonate groups that show O \cdots H interactions, only two out of the three oxygen atoms participate in these types of contacts. The remaining protonated oxygen atoms take part in H \cdots O interactions, which make up 11.7 and 10.8% of the Hirshfeld surfaces of calixarenes A and B, respectively. On calixarene A, these contacts are due to the protonated hydroxyl interacting with either an oxygen atom from a water molecule, or a deprotonated hydroxyl group from a neighboring calixarene. However, on calixarene B these interactions are restricted to the interaction of a protonated hydroxyl and an oxygen atom from a close water molecule.

Structure **5c** is different from **5b** in that two of the six phosphonate ligands are completely deprotonated and there is only one calixarene in the asymmetric unit. C \cdots H interactions comprise 7.4% of the Hirshfeld surface for the calix-[6]arene and are notable for a lack of short contacts. The shortest contact is where methylene protons from a neighboring calixarene points into a phenyl ring of the calixarene. O \cdots H contacts make up 29.3% of the surface of the calix-[6]arene and are represented by the large spike in the bottom left-hand corner of the plot, Figure 9A. As in **5b**, four of the six phosphonate groups display O \cdots H interactions, with the two completely deprotonated phosphonate ligands displaying only O \cdots H interactions, Figure 10. Contacts between deprotonated hydroxyl groups and water molecules, or deprotonated hydroxyl groups and protonated phosphonate groups comprise the majority of these interactions; however, there are contacts between phenolic oxygen atoms and bound water molecules which also contribute.

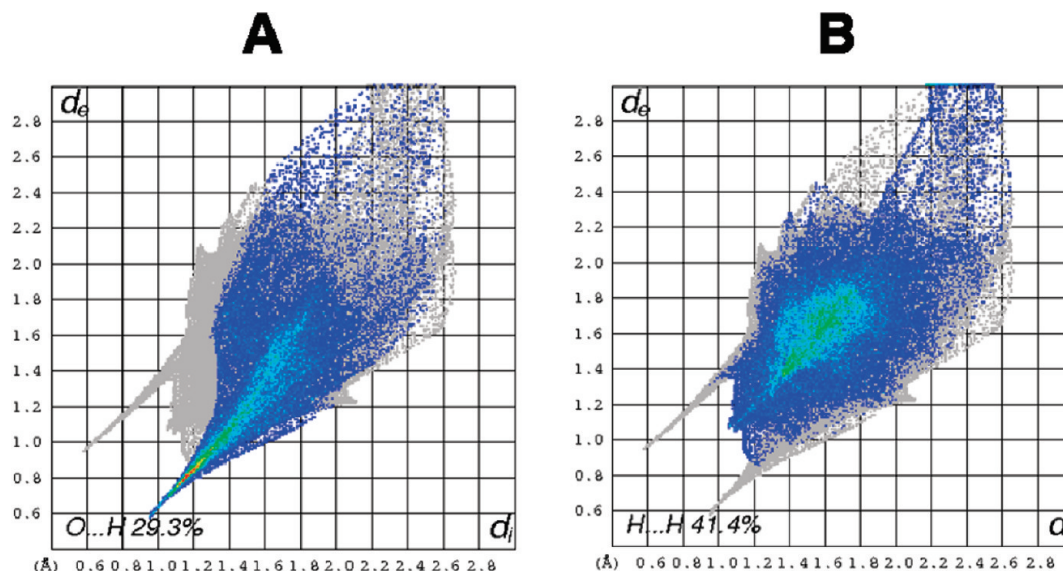


Figure 9. Fingerprint plots of the calixarene molecule in complex **5c**: (A) O...H interactions and (B) H...H interactions.

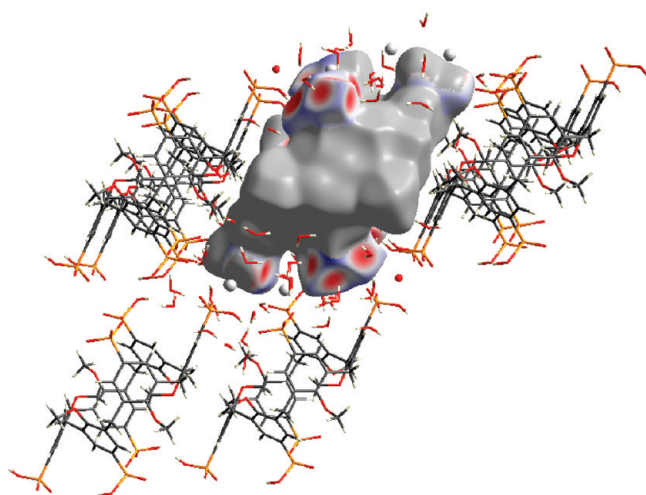


Figure 10. View of the O...H interactions for the calixarene molecule in complex **5c**, with red areas highlighting short contacts.

For the six phosphonate groups, four of them participate in O...H bonding; however, the other two are involved in O...Ca interactions, with similar contacts to the O...Ca interactions seen in **5b**, Figure 11. These O...Ca interactions make up 5.7% of the Hirshfeld surface. Noteworthy is that in the other four phosphonate groups there are four short contacts, each corresponding to a calcium atom which bridges two of these phosphonate groups. This feature is not observed in structure **5b**.

The majority of the surface is made up of H...H contacts, which account for 41.4% of the Hirshfeld surface, Figure 9B. An interesting feature of the fingerprint plot is the “double spike”, seen toward the bottom left of the plot where $d_e \approx d_i$. This is due to the interaction of a hydrogen from the O-methyl group of the calixarene with a meta hydrogen from a neighboring calixarene. The atoms are not a uniform distance away from the Hirshfeld surface generated and are manifested in the “double spike” in the plot.

Previously, we have reported that a series of *p*-phosphonic acid calix[*n*]arenes ($n = 4, 5, 6$, and 8) form stable nanoarrays (nanoparticles) or nanorfts ($n = 4$) in the gas phase using

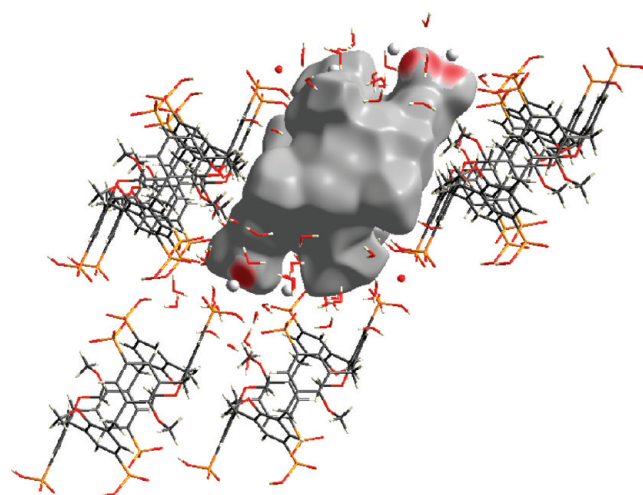


Figure 11. View of the O...Ca interactions for the calixarene molecule in complex **5c**, with red areas highlighting short contacts.

MALDI-TOF-MS with around 20 calixarene units (18–30 kDa) per nanoarray.⁸ This has been extended to alkylated *p*-phosphonic acid calix[4]arenes with successive peaks out to 15, 33, and 16 calixarene units for the methyl, butyl, and octadecyl derivatives, respectively.⁹ MALDI-TOF-MS of methylated *p*-phosphonic acid calix[6]arene, Figure 12, shows nanoarrays up to 28 calixarene units in size. Presumably this association arises also from the multiple hydrogen bonding between calixarenes through the phosphonic acid moieties as in the well-characterized structures of the *p*-phosphonic acid calix[4]arene, and its calcium complexes,¹² and also interactions between the aromatic rings ($\pi \cdots \pi$ and $\pi \cdots \text{H}-\text{O}$). Interestingly, all these structure form bilayers with the calixarene in the “up–down” arrangement, and it is therefore likely that the parent O-methylated calix[4]arene in the present study is also assembled into bilayers, and for the calcium complexes reported herein, that it also assembles into bilayers, and these are persistent to a degree in the gas phase. This is also consistent with the closely related *p*-sulfonated calix[6]arene also assembling into bilayers with the calixarenes in the “up–down” arrangement.¹⁹

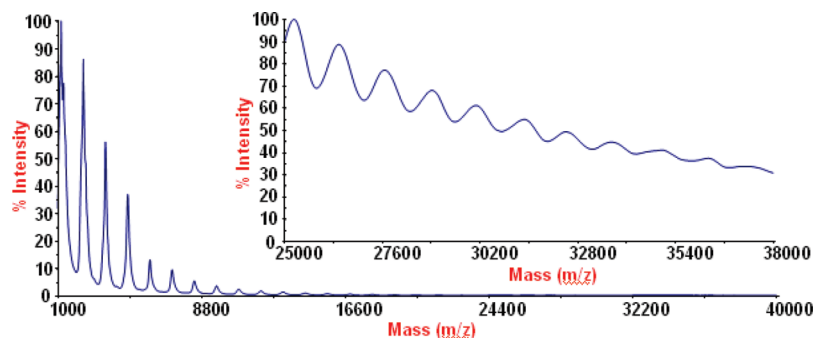


Figure 12. MALDI-TOF-MS showing nanoarrays for *p*-phosphonic acid hexamethoxy-calix[6]arene.

Conclusion

We have synthesized the novel compound *p*-phosphonic acid hexamethoxy-calix[6]arene in three steps starting from hexamethoxy-calix[6]arene with 57% overall yield. The hexaphosphonic acid shows nanoarray formation in the gas phase with up to 28 calixarene units per array. This is analogous to the calix[4]arene phosphonic acids that are either nonalkylated or alkylated at the lower rim and form nanoarrays between 15 and 33 calixarene units in size. A pattern is now emerging in that the phosphonic acid upper rim groups of calixarenes are effective in assembling the molecules into assemblies, regardless of the nature of the O-alkyl group, or the absence of such a group, and this relates to each functional group being able to contribute to O–H groups in forming complex hydrogen bonding arrays. This is distinctly different from the ubiquitous sulfonated calixarenes, where each function group has only one O–H moiety, and hence less extensive hydrogen bonding capability. The hexaphosphonic acid forms two different calcium complexes with extended polymeric layers in the solid state with calcium ions and waters of sandwiched between layers of calixarenes. The different ratio of calcium to calixarene in these complexes, and for *p*-phosphonic acid calixarene itself,⁸ also highlights another pattern for phosphonic acid calixarenes, namely, the variability of uptake/binding of metal ions arising from different degrees of deprotonation of the phosphonic acid moieties and suggests a plethora of different metal ion complexes for phosphonated calixarenes in general. The new calcium complexes have potential uses as calcium delivery systems in the human body and in understanding cation–carrier interactions.

Experimental Section

Materials and Methods. All starting materials and solvents were obtained from commercial suppliers and used without further purification except otherwise noted. Acetonitrile was dried over 4 Å molecular sieves for 24 h and NiCl₂·6H₂O was dried at 180 °C in vacuo for 8 h before use. All moisture-sensitive reactions were performed under a positive pressure of nitrogen. Chromatographic purification was performed using 200–400 mesh silica gel. Thin layer chromatography (TLC) analysis was performed on silica gel plates (absorbent thickness 250 μm) containing a fluorescent indicator. Melting points were determined using sealed and evacuated capillary tubes on an Electrothermal 9100 melting point apparatus and are uncorrected. IR spectra were recorded as KBr pellets on a Perkin-Elmer Spectrum One spectrometer. ¹H NMR (500 MHz), ¹³C NMR (126 MHz), and ³¹P NMR (202 MHz) were recorded on a Bruker spectrometer and internally referenced to the solvent signal or phosphoric acid for ³¹P NMR. Elemental analysis was performed at The Campbell Microanalytical Laboratory, Otago, New Zealand and FAB-MS was performed on a HP5896 mass spectrometer.

Matrix assisted laser desorption ionization time-of-flight mass spectrometry (MALDI-TOF-MS) experiments were conducted on an Applied Biosystems Voyager DE-STR mass spectrometer. Data were collected in the negative ion, linear mode with delayed extraction. The accelerating voltage was set at 25 kV, and delay time was 500 ns with the low mass gate set at 500 Da. Each spectrum was an average of 1000 shots. A standard mixture of five peptides of mass range from 1000 to 6000 Da was used for external calibration. *p*-Phosphonic acid hexamethoxy-calix[6]arene was dissolved in methanol to a final concentration of 1 mM and premixed with 2,5-DHB (150 mg/mL in 50% (v/v) methanol) at a ratio of 1:1. A 1-μL volume of the premixed solution was deposited onto a stainless steel 100-well MALDI target plate (Applied Biosystems) and allowed to air-dry at room temperature.

Calix[6]arene, **1**,¹⁵ and hexamethoxycalix[6]arene, **2**,¹⁶ were prepared as described previously in the literature.

5,11,17,23,29,35-Hexaiodo-37,38,39,40,41,42-hexamethoxycalix[6]arene (3). A suspension of 1.84 g (8.32 mmol) of CF₃CO₂Ag and 0.50 g (0.69 mmol) of **2** was refluxed in 50 mL of chloroform for 4 h. After this time 4.23 g (16.65 mmol) of I₂ was added and the purple solution was refluxed for a further 2 h. After being cooled to RT, the mixture was filtered over Celite and the filtrate was washed with a saturated solution of Na₂S₂O₅ (2 × 10 mL) and then water (3 × 10 mL). The organic layer was dried over MgSO₄, filtered, and evaporated under reduced pressure to yield 0.68 g (66%) of **3** as a pale yellow solid. Trituration with dimethylformamide yielded **3** as a pure white solid suitable for microanalysis. mp > 260 °C (dec.); ¹H NMR (CDCl₃, 25 °C, 500 MHz) δ 7.24 (s, 12H, *m-H*), 3.83 (s, 12H, ArCH₂Ar), 3.35 (s, 18H, OCH₃); ¹³C NMR (CDCl₃, 25 °C, 126 MHz) δ 156.41, 138.00, 136.71, 87.97, 60.76, 29.79; HRMS (FAB) *m/z* calcd for (C₄₈H₄₂I₆O₆)⁺ 1475.7250, found 1475.7196; Anal. Calcd for C₄₈H₄₂I₆O₆: C 39.05, H 2.87, found: C 39.13, H 3.07.

5,11,17,23,29,35-Hexa(diethoxyphosphoryl)-37,38,39,40,41,42-hexamethoxycalix[6]arene (4). A solution of 1.50 g (1.02 mmol) of **3** and 0.20 g (1.53 mmol) of NiCl₂ in 40 mL of benzonitrile (not completely soluble) was treated dropwise with 2.61 mL (15.25 mmol) of P(OEt)₃ under nitrogen at 180 °C. The solution was stirred for 0.5 h and the volatiles were removed under reduced pressure to leave an orange residue. The residue was dissolved in 100 mL of toluene, washed with 5% ammonia solution (5 × 30 mL), dried over MgSO₄, and evaporated under reduced pressure to yield an orange oil. The oil was chromatographed over silica gel to yield 1.44 g (92%) of **4** as a white solid. Recrystallization from toluene yielded X-ray quality single crystals, **4a**, which were also submitted for microanalysis. *R*_f 0.35 (1:19 methanol-dichloromethane); mp 236–237 °C; IR (KBr) 2984 (m), 2907 (m), 1638 (w), 1593 (w), 1472 (m), 1272 (s), 1020 (s), 966 (s), 794 (m), 548 (m) cm⁻¹; ¹H NMR (CDCl₃, 25 °C, 500 MHz) δ 7.40 (d, 12H, ArH, *J*_{P–H} = 13.5 Hz), 4.09–4.01 (m, 12H, POCH₂CH₃), 4.01–3.93 (m, 12H, POCH₂CH₃), 3.96 (s, 12H, ArCH₂Ar), 3.30 (s, 18H, OCH₃), 1.22 (t, 36H, POCH₂CH₃, *J* = 7.0 Hz); ¹³C NMR (CDCl₃, 25 °C, 126 MHz) δ 159.71 (d, ⁴*J*_{P–C} = 3.8 Hz), 134.63 (d, ³*J*_{P–C} = 16.0 Hz), 132.82 (d, ²*J*_{P–C} = 10.8 Hz), 123.24 (d, ¹*J*_{P–C} = 189.8 Hz), 62.19 (d, ²*J*_{P–C} = 5.5 Hz), 60.39, 30.02, 16.24 (d, ³*J*_{P–C} = 6.4 Hz); ³¹P NMR (CDCl₃, 25 °C, 202 MHz) δ 19.26; HRMS (FAB) *m/z* calcd for (C₇₂H₁₀₂O₂₄P₆ + H)⁺ 1537.5265, found 1537.5202; Anal. Calcd for C₇₂H₁₀₂O₂₄P₆ + H₂O: C 55.60, H 6.74, found: C 55.40, H 6.53.

5,11,17,23,29,35-Hexa(dihydroxyphosphoryl)-37,38,39,40,41,42-hexamethoxycalix[6]arene (5). 2.89 mL (21.87 mmol) of bromotrimethylsilane was added to 1.40 g (0.91 mmol) of **4** in 50 mL of dry acetonitrile and the solution was refluxed for 16 h. The volatiles were removed under reduced pressure and the resulting residue was triturated with 30 mL of acetonitrile and 1 mL of water. The precipitate formed was filtered off, washed with acetonitrile (3 × 10 mL), and recrystallized from methanol to yield 1.04 g (95%) of **5** as a white solid. Recrystallization from methanol/6 M HNO₃/CsNO₃ yielded X-ray quality crystals, **5a**, which were also submitted for microanalysis. mp > 280 °C (dec); IR (KBr) 3180 (br), 2937 (m), 2834 (m), 2300 (br), 1641 (w), 1595 (w), 1472 (m), 1272 (m), 1118 (s), 1003 (s), 965 (s), 516 (m) cm⁻¹; ¹H NMR (DMSO-*d*₆, 25 °C, 500 MHz) δ7.28 (d, 12H, ArH, *J*_{P-H} = 13.2 Hz), 6.60 (br s, POH, shifts downfield with increasing [H]⁺), 3.96 (s, 12H, ArCH₂-Ar), 3.13 (s, 18H, OCH₃); ¹³C NMR (DMSO-*d*₆, 25 °C, 126 MHz) δ158.12, 133.93 (d, ³*J*_{P-C} = 15.5 Hz), 131.38, 128.47 (d, ¹*J*_{P-C} = 186.0 Hz), 59.92, 29.92; ³¹P NMR (DMSO-*d*₆, 25 °C, 202 MHz) δ15.17; HRMS (FAB) *m/z* calcd for (C₄₈H₅₄O₂₄P₆)⁺ 1200.1431, found 1200.1491; Anal. Calcd for C₄₈H₅₄O₂₄P₆ + 0.55HNO₃ + 0.1H₂O: C 46.60, H 4.46, found: C 46.61, H 4.44.

X-ray Crystallography. Suitable crystals of **5a** and **5b** for diffraction studies were prepared by dissolving 4.2 mmol of **5** and 11.4 (for **5a**) or 17.0 (for **5b**) mmol of Ca(acetate)₂·H₂O in 2 mL of water close to reflux, followed by filtration, cooling to room temperature, followed by slow evaporation over several days. Uniformity of the samples was checked by cell determinations of several crystals for each sample. The X-ray diffracted intensities were measured from single crystals on one of two machines. The first machine was an Oxford Diffraction Gemini-R Ultra CCD diffractometer at about 100 K using monochromatized Cu-K_α (λ = 1.54178 Å). The second machine was a Bruker ASX SMART CCD diffractometer at about 100 or 153 K using monochromatized Mo-K_α (λ = 0.71073 Å). Data were corrected for Lorentz and polarization effects and absorption correction applied using multiple symmetry equivalent reflections. The structures were solved by direct method and refined on *F*² using the SHELX-97 crystallographic package¹⁷ and X-seed interface.¹⁸ A full matrix least-squares refinement procedure was used, minimizing $w(F_o^2 - F_c^2)$, with $w = [\sigma^2(F_o^2) + (AP)^2 + BP]^1$, where $P = (F_o^2 + 2F_c^2)/3$. Agreement factors ($R = \sum |F_o| - |F_c| / \sum |F_o|$, $wR2 = \{\sum [w(F_o^2 - F_c^2)^2] / \sum [w(F_o^2)^2]\}^{1/2}$ and $GOF = \{\sum [w(F_o^2 - F_c^2)^2] / (n - p)\}^{1/2}$ are cited, where *n* is the number of reflections and *p* is the total number of parameters refined). All non-hydrogen atoms were refined anisotropically. The positions of hydrogen atoms partly were localized from the difference Fourier map, partly calculated from geometrical consideration, and their atomic parameters were constrained to the bonded atoms during the refinement. CCDC deposition numbers 766115–766116, 766252–766253.

Crystal/refinement details for complex **4a**: C₇₂H₁₀₄O₂₅P₆, *M* = 1555.37, *F*(000) = 6608 *e*, monoclinic, *C*2/*c* (No. 15), *Z* = 8, *T* = 153(2) K, *a* = 40.464(5), *b* = 17.430(2), *c* = 27.483(4) Å, β = 123.113(1)°, *V* = 16235(4) Å³, *D*_c = 1.273 g cm⁻³, μ_{Mo} = 0.205 mm⁻¹, sin θ/λ_{max} = 0.5946, *N*(unique) = 13879 (merged from 49484, *R*_{int} = 0.0311, *R*_{sig} = 0.0339), *N*_o (*I* > 2σ(*I*)) = 9507, *R* = 0.1489, *wR*2 = 0.3559 (*A*, *B* = 0.15, 190.0), *GOF* = 1.041, |Δρ_{max}| = 2.1(1) e Å⁻³.

Crystal/refinement details for complex **5a**: C₄₈H₇₀N₄O₄₂P₆, *M* = 1560.90, *F*(000) = 812 *e*, triclinic, *P*1̄ (No. 2), *Z* = 1, *T* = 100(2) K, *a* = 12.182(2), *b* = 12.332(2), *c* = 13.108(2) Å, α = 113.447(3), β = 94.212(3), γ = 108.695(3)°, *V* = 1664.9(5) Å³, *D*_c = 1.557 g cm⁻³, μ_{Mo} = 0.270 mm⁻¹, sin θ/λ_{max} = 0.5946, *N*(unique) = 5816 (merged from 10181, *R*_{int} = 0.0251, *R*_{sig} = 0.0465), *N*_o (*I* > 2σ(*I*)) = 4259, *R* = 0.0697, *wR*2 = 0.1849 (*A*, *B* = 0.10, 3.70), *GOF* = 1.054, |Δρ_{max}| = 1.1(1) e Å⁻³.

Crystal/refinement details for complex **5b**: C₄₈H₁₀₄Ca₃O₅₂P₆, *M* = 1819.37, *F*(000) = 1916 *e*, triclinic, *P*1̄ (No. 2), *Z* = 2, *T* = 100(2) K,

a = 14.0340(4), *b* = 16.2130(5), *c* = 19.4062(6) Å, α = 110.878(3), β = 95.287(2), γ = 99.200(2)°, *V* = 4019.0(2) Å³, *D*_c = 1.503 g cm⁻³, sin θ/λ_{max} = 0.5981, *N*(unique) = 14088 (merged from 42363, *R*_{int} = 0.0499, *R*_{sig} = 0.0770), *N*_o (*I* > 2σ(*I*)) = 8081, *R* = 0.0362, *wR*2 = 0.0704 (*A*, *B* = 0.024, 0), *GOF* = 1.004, |Δρ_{max}| = 0.55(6) e Å⁻³.

Crystal/refinement details for complex **5c**: C₄₈H₉₉Ca₄O_{50.5}P₆, *M* = 1830.41, *F*(000) = 961 *e*, triclinic, *P*1̄ (No. 2), *Z* = 1, *T* = 100(2) K, *a* = 11.4113(7), *b* = 12.9903(9), *c* = 15.4684(11) Å, α = 112.047(7), β = 95.814(5), γ = 108.467(6)°, *V* = 1951.6(2) Å³, *D*_c = 1.557 g cm⁻³, sin θ/λ_{max} = 0.5984, *N*(unique) = 6828 (merged from 22732, *R*_{int} = 0.0977, *R*_{sig} = 0.1485), *N*_o (*I* > 2σ(*I*)) = 3372, *R* = 0.0495, *wR*2 = 0.0942 (*A*, *B* = 0.025, 0), *GOF* = 1.008, |Δρ_{max}| = 1.30(8) e Å⁻³.

Acknowledgment. We thank the ARC, NSF, and NIH (Grant P41RR000954) for financial support of this work and the University of Western Australia for SIRF, GRST, and PRT awards to TEC.

Supporting Information Available: Crystallographic information file (cif). This material is available free of charge via the Internet at <http://pubs.acs.org>.

References

- (1) Diamond, D.; McKerverve, M. A. *Chem. Soc. Rev.* **1996**, *25*, 15–24.
- (2) (a) Atwood, J. L.; Barbour, L. J.; Jerga, A. *Science* **2002**, *296*, 2367–2369. (b) Atwood, J. L.; Dalgarno, S. J.; Thallapally, P. K. *J. Am. Chem. Soc.* **2006**, *128*, 15060–15061.
- (3) Atwood, J. L.; Koutsantonis, G. A.; Raston, C. L. *Nature* **1994**, *368*, 229–231.
- (4) Kotek, J.; Lukes, I.; Plutnar, J.; Rohovec, J.; Zak, Z. *Inorg. Chim. Acta* **2002**, *335*, 9.
- (5) (a) Atwood, J. L.; Bott, S. G.; Hamada, F.; Means, C.; Orr, G. W.; Robinson, K. D.; Zhang, H. *Inorg. Chem.* **1992**, *31*, 603–607. (b) Atwood, J. L.; Barbour, L. J.; Orr, G. W. *Science* **1999**, *285*, 1049–1052. (c) Hardie, M. J.; Raston, C. L. *J. Chem. Soc., Dalton Trans.* **2000**, 2483–2492.
- (6) (a) Clark, T. E.; Makha, M.; McKinnon, J. J.; Raston, C. L.; Sobolev, A. N.; Spackman, M. A. *CrystEngComm* **2007**, *9*, 566–569. (b) Coleman, A. W.; Kuduva, S. S.; Shahgaldian, P.; Zaworotko, M. J. *Chem. Commun.* **2005**, 1968–1970.
- (7) Arduini, A.; Casnati, A. *Macrocyclic Synthesis*, 1st ed.; Oxford University Press: Oxford, 1996.
- (8) (a) Clark, T. E.; Makha, M.; Sobolev, A. N.; Su, D.; Rohrs, H.; Gross, M. L.; Atwood, J. L.; Raston, C. L. *New J. Chem.* **2008**, *32*, 1478–1483. (b) Clark, T. E.; Makha, M.; Sobolev, A. N.; Rohrs, H.; Atwood, J. L.; Raston, C. L. *Eur. J. Chem.* **2008**, *14*, 3931–3938.
- (9) Clark, T. E.; Makha, M.; Sobolev, A. N.; Su, D.; Rohrs, H.; Gross, M. L.; Raston, C. L. *Cryst. Growth Des.* **2009**, *9*, 3575–3580.
- (10) Cheng, B.; Mattson, M. P. *J. Neurosci.* **1992**, *12*, 1558–1666.
- (11) Thackery, E. *The Gale Encyclopedia of Cancer*, 1st ed.; The Gale Group: Farmington Hills, MI, 2002.
- (12) Martin, A. D.; Raston, C. L.; Sobolev, A. N.; Spackman, M. A. *Cryst. Growth Des.* **2009**, *9*, 3759–3764.
- (13) (a) Clark, T. E.; Makha, M.; Sobolev, A. N.; Raston, C. L. *Cryst. Growth Des.* **2008**, *8*, 890–896. (b) Jayatilaka, D.; Spackman, M. A. *Cryst. Eng. Comm.* **2009**, *11*, 19–32.
- (14) Jayatilaka, D.; McKinnon, J. J.; Spackman, M. A. *Chem. Commun.* **2007**, 3814–3816.
- (15) Parker, D., Ed. *Macrocyclic Synthesis: A Practical Approach*; Oxford University Press: Oxford, 1996.
- (16) Gutsche, C. D.; Lin, L. *Tetrahedron* **1986**, *42*, 1633.
- (17) Sheldrick, G. M. *Acta Crystallogr.* **2008**, *A64*, 3.
- (18) Barbour, L. J. *J. Supramol. Chem.* **2001**, *1*, 189.
- (19) Dalgarno, S. J.; Hardie, M. J.; Makha, M.; Raston, C. L. *Chem.—Eur. J.* **2003**, *9*, 2384.